

PROCEEDINGS OF SPIE

SPIDigitalLibrary.org/conference-proceedings-of-spie

Highly-sensitive anisotropic porous silicon based optical sensors

Jesús Álvarez, Paolo Bettotti, Neeraj Kumar, Isaac Suárez, Daniel Hill, et al.

Jesús Álvarez, Paolo Bettotti, Neeraj Kumar, Isaac Suárez, Daniel Hill, Juan Martínez-Pastor, "Highly-sensitive anisotropic porous silicon based optical sensors," Proc. SPIE 8212, Frontiers in Biological Detection: From Nanosensors to Systems IV, 821209 (31 January 2012); doi: 10.1117/12.908214

SPIE.

Event: SPIE BiOS, 2012, San Francisco, California, United States

Highly-sensitive anisotropic Porous Silicon based optical sensors

Jesús Álvarez^{*a}, Paolo Bettotti^b, Neeraj Kumar^b, Isaac Suárez^a, Daniel Hill^a,
and Juan Martínez-Pastor^a

^aUMDO, Materials Science Institute, University of Valencia, P.O. Box 22085, 46071
Valencia, Spain

^bNanoscience Laboratory, Department of Physics, University of Trento, via Sommarive 14, 38050
Povo-Trento, Italy

ABSTRACT

The modeling, fabrication and characterization of PSi fabricated from both (110) and (100) surface oriented silicon for optical sensing is thoroughly reported. First, based on the generalized Bruggeman method, the birefringence and sensitivity of the fabricated membranes were calculated as a function of the fabrication parameters such as porosity and pore sizes; and external effects, such as the pores surface oxidation. Thereafter we report on the fabrication of PSi membranes from (110) and (100) surface oriented silicon with pore sizes in the range of 50 – 80 nm, and the characterization of their birefringence using a polarimetric setup. Their sensitivities were determined by filling the pores with several liquids having different refractive index. As a result, sensitivities as high as 1407 nm/RIU were obtained for the (110) samples at a 1500 nm wavelength and 382 nm/RIU for the (100) samples at the same wavelength.

Keywords: Porous silicon, birefringence, phase retardation, optical sensor.

1. INTRODUCTION

Nowadays there is an increasing need of developing biological sensors for medical, environmental monitoring, food safety and research applications [1]. Porous Silicon (PSi) has unique properties for the development of these sensors since its huge surface/volume ratio enables the capture of greater amounts of the target molecules than planar sensors. Moreover, its porosity, thickness and pore diameters can be tuned by changing the etching conditions during the fabrication process. Up to now, several interferometric schemes using PSi have been proposed for the realization of chemical and biological sensors [2-5]. Other works [6-8] have demonstrated experimentally the possibility of using PSi made from (110) wafer for sensing applications due to the fact that this orientation presents a very high birefringence, being it possible to detect different substances within its pores by means of the changes of this value. The use of this anisotropic PSi together with optical polarimetric schemes for measurement of phase retardation therefore makes it an ideal candidate for commercially viable highly sensitive optical sensors.

In this work, based on the theoretical approach developed previously in [9-10] the theoretical optical properties of PSi fabricated from (110) and (100) silicon substrates is studied. For this purpose the binary Bruggeman model [16] is extended by including an important external effect in PSi like silicon oxidation. Then, the measured birefringence values for samples filled with several liquids are compared with the theoretical ones obtained using this extended model. Lastly the measured birefringence and sensitivity for both type of samples (110) and (100) are evaluated and compared. Thereafter we report on the fabrication of several PSi membranes from both types of substrates. Using two different polarimetric setups the birefringence and sensitivity of the fabricated samples are determined; a bulk refractive index sensitivity of 1407 nm/RIU comparable to the 1525 nm/RIU predicted by the theory is reported.

*jesus.alvarez@uv.es; phone 0034963544875; fax 0034963543633; www.uv.es/umdo

2. THEORY

PSi prepared from (110) Si surface oriented substrates presents a high anisotropy due to pores grow preferentially along the [100] and [010] crystallographic directions [12]. The orientation of the pores along those directions results in a difference in the refractive indices along the [001] and the [110] directions [13]. In accounting for the anisotropic microstructure of this type of PSi, the pores are modeled as ellipsoids of revolution with their axes of symmetry aligned along the [001] direction and the [110] direction lying on the (110) surface plane. The depolarization tensor factors, L_e and L_o , describe the screening efficiency of external electromagnetic fields inside the ellipsoids, characterizing the optical properties of the PSi layer. As the directions [100] and [010] form an angle of 50.77° with respect to the normal plane (110) [14], the depolarization tensor factors are: L_e equal to 0.2938 and L_o equal to 0.4035.

For the case of PSi prepared from (100) surface oriented silicon, the pores are modeled as cylinders oriented in the [100] direction. For cylindrical pores the depolarization factor tensors have values of L_e equal to 0.5 and L_o equal to 0 [15].

Using the generalized Bruggeman model [16] the birefringence can be obtained as a function of the fabrication parameters such as porosity and refractive index of the material that fills the pores. The only assumption made by this model is the static electric field condition, which is satisfied when the wavelength of light is much longer than the pore diameter. That is the case of the presented in this work, where the pore diameters are in the range of 50-80nm. The Bruggeman model is described by:

$$\sum_i f_i \frac{n_i^2(\lambda) - n_{e,o}^2}{n_{e,o}^2 + L_{e,o} \cdot (n_i^2(\lambda) - n_{e,o}^2)} = 0 \quad (1)$$

where f_i is the volume fraction of the different materials that form the PSi membrane, $n_i(\lambda)$ the refractive indices, and L_e and L_o the previously described depolarization tensor factors. The unknown n_e and n_o are the refractive indices along the main axes of the pore and the birefringence is obtained by its difference $\Delta n = n_e - n_o$. Then, solving Equation 1 with numerical methods we obtained the theoretical birefringence values as a function of the porosity considering different pore refractive indexes. These results are depicted in Figure 1 for both (110) and (100) PSi samples.

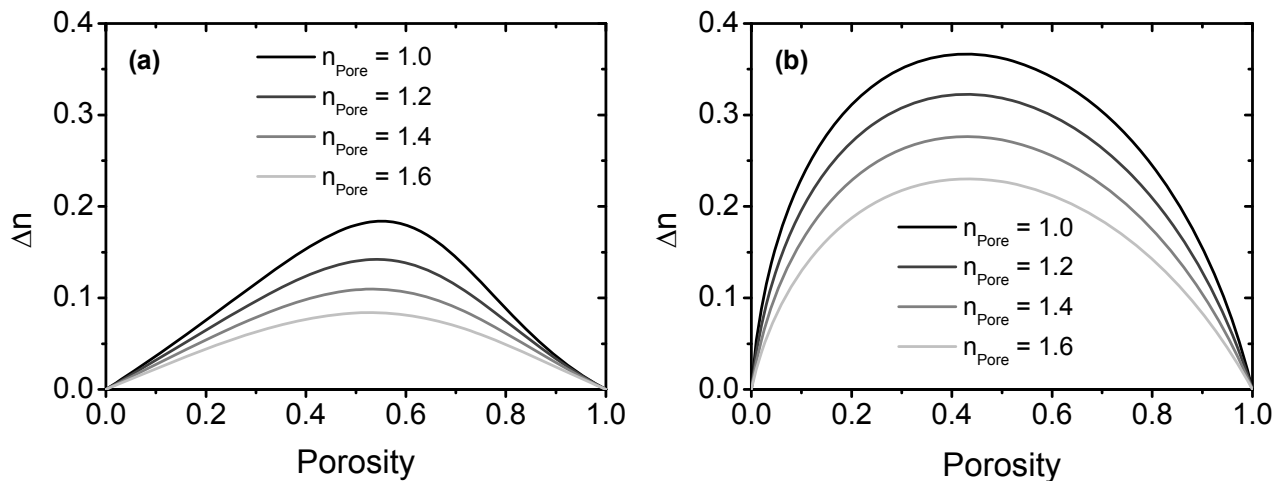


Figure 1. Birefringence as a function of the PSi layer porosity considering several refractive index of the material that fills the pores for a (110) sample (a) and (100) sample (b).

Figure 1 shows that birefringence presents a maximum value for a porosity of 0.55 in the case of the (110) PSi and 0.45 for the (100) samples. Also, for both type of samples the birefringence decreases with the refractive index contrast between the silicon and the material filling the pores. That is transducer mechanism of anisotropic porous silicon to be used an optical sensor: variations in the refractive index of material filling the pores will modify the global birefringence of the sample. From Figure 1, we can also see that the birefringence increase is optimized in the cases where when the initial birefringence achieves its maximum value, so we can conclude that for having an efficient sensing mechanism the birefringence should be as high as the fabrication process makes it possible.

2.1 Effect of silicon oxidation

The internal pore surfaces of freshly prepared PSi are prone to oxidize under ambient conditions leaving a thin SiO₂ layer over recently etched PSi pores. This oxidation process continues over time changing the optical properties of the PSi, so a method to stabilize the pores surface is needed in order to avoid this change in the optical properties. One of the simplest solutions for the surface stabilization is to purposely increase this silicon dioxide layer via a thermal oxidation process [17]. The silicon dioxide need to be taken into account to give accurate prediction of the theoretical birefringence and sensitivity values. This can be done by including the volume of the silicon dioxide layer in Equation 1. Thus, a three component medium has now been formed consisting of silicon, silicon dioxide and pores. The bonding of silicon with oxygen produces a 2.27 fold increase in volume over bulk silicon, so silicon oxidation produces a reduction of pores and silicon volume fractions [18]. The new volume fractions of silicon and pores are related to the silicon dioxide volume fraction by Equations. 2 and 3 respectively:

$$f_{Si} = f_{Si_0} - f_{SiO_2} / 2.27; \quad f_{Pores} = f_{Pores_0} - 1.27 / 2.27 \cdot f_{SiO_2} \quad (2), (3)$$

where f_{Si_0} and f_{Pores_0} denotes the volume fraction of the silicon and pores prior to oxidation. The effect that grown silicon dioxide has over the birefringence is depicted in Figure 2. As can be seen, silicon dioxide reduces the birefringence for both types of samples. This reduction in birefringence is attributed to the decrease of the index contrast between the initial PSi layer, and the same layer after the oxidation process.

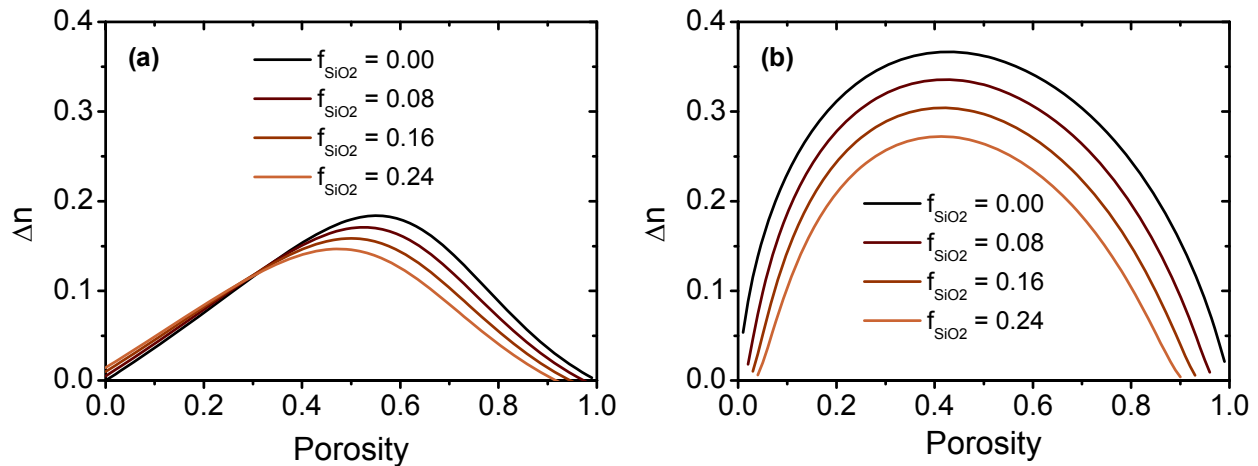


Figure 2. Birefringence as a function of the PSi layer porosity for several silicon dioxide volume fractions for a (110) sample (a) and (100) sample (b).

3. FABRICATION

The set of the fabricated samples from (110) surface oriented silicon consisted of mesoporous silicon etched into n-type Si with resistivity of 0.01-0.001 Ohm/cm. Pores sizes were around 50 nanometers, as shown in Figure 3 (a). Samples were prepared by electrochemical etching using a solution composed of HF:Ethanol=3:7 by volume, considering an initial HF concentration of 48%. A current density of 25 mA/cm² was used during the etching.

The other set of samples, prepared from (100) surface oriented silicon, consisted of mesoporous silicon etched into p-type Si with resistivity of 0.01-0.001 Ohm/cm. In this case the pore sizes were around 80 nanometers, as shown in Figure 3 (b).

For subsequent optical characterization, porous membranes were detached from the bulk silicon layer that supports them by applying a strong current burst at the end of the etching completely dissolving the bottom silicon layer that surrounds the etched area. With this procedure the membrane can be transferred to another substrate. More details can be found in [19].

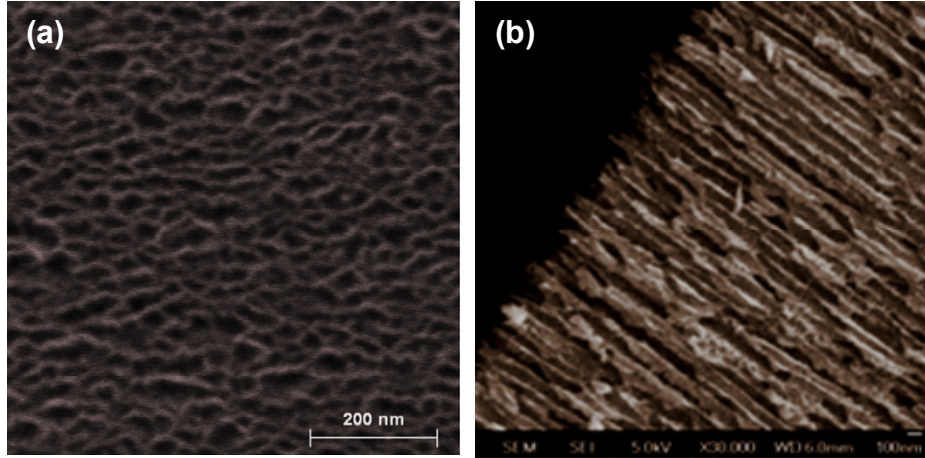


Figure 3. (a) Surface SEM image of the fabricated sample from (110) surface oriented silicon. Pore diameter is around 50 nm. (b) Cross section SEM image of the fabricated sample from (100) surface oriented silicon. Pore diameters are around 80 nm.

4. EXPERIMENTAL AND RESULTS

The optical anisotropy of the samples was determined by analyzing the state of polarization of the light transmitted through them. Since the two types of samples have different properties, as it will be show in the next subsections, two different polarimetric setups were employed to determine the birefringence and sensitivity.

4.1 PSi made from (110) substrate

For this type of samples, the birefringence was determined by using a tungsten halogen lamp and two spectrometers to record the phase retardation as a function of the wavelength in the range from 600 nm to 1600 nm. The phase retardation is related to the samples birefringence by means of:

$$\Delta\phi(\lambda) = \frac{2\pi}{\lambda} \cdot d \cdot \Delta n(\lambda) \quad (4)$$

where λ is the incident wavelength of light, d the PSi membrane thickness and $\Delta n(\lambda)$ its birefringence.

The output light from a tungsten halogen lamp is collimated and then polarized linearly at 45° with respect to the horizontal direction. The linearly polarized light passes through the anisotropic PSi sample which is oriented with its [001] and $[\bar{1}\bar{1}0]$ crystallographic directions parallel to the vertical and horizontal directions, respectively. The phase shift is converted into an amplitude shift through traversing a second polarizer (usually called analyzer), which is then recorded by the spectrometers. The analyzer is placed parallel and crossed with respect to the first polarizer, so the ratio of the transmitted linearly polarizer light components, $R(\lambda)$, is obtained by dividing the spectrum measured when the polarizers are crossed by the one obtained when the polarizers are placed in parallel. The relation between the phase retardation and $R(\lambda)$ is given by:

$$R(\lambda) = \frac{T_{\perp}(\lambda)}{T_{\parallel}(\lambda)} = \frac{\sin^2(\Delta\phi(\lambda)/2)}{\cos^2(\Delta\phi(\lambda)/2)} \quad (5)$$

So, using the previously described method, $R(\lambda)$ were obtained for a $42 \mu\text{m}$ sample thick when its pores were filled with air, and then with different liquids such as water ($n_{\text{Water}} \approx 1.33$), ethanol ($n_{\text{Ethanol}} \approx 1.36$) and isopropanol ($n_{\text{Isop}} \approx 1.377$). Figure 4 (a) shows the values of $R(\lambda)$ recorded in the range of 600 nm – 1600 nm for the previously cited cases. A blue-shift can clearly be seen from the sample filled when the pores are filled with liquids. From the position of the zeros and poles of $R(\lambda)$, the birefringence values for the four cases were obtained as a function of the wavelength by using Equations (5) and (6) to relate the position of the poles and zeros with the phase retardation, and consequently with the

birefringence. Figure 4 (b) depicts the obtained values of the birefringence under the four different conditions of the sample, voids pores (gray dots), pores filled with water (blue dots), ethanol (green line) and isopropanol (orange line).

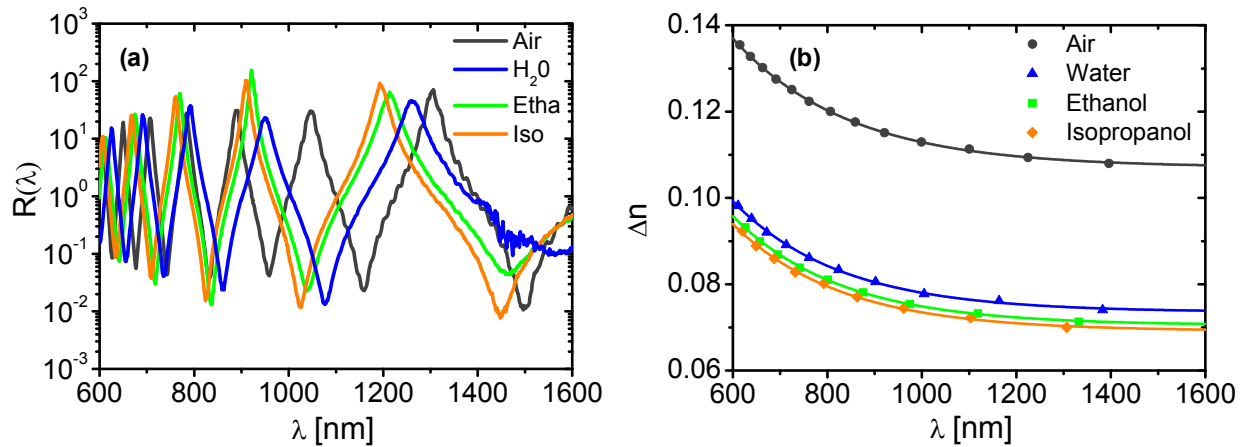


Figure 4. (a) Measured $R(\lambda)$ from a 42 μm thick (110) PSi sample for: empty pores (gray line), pores filled with water (blue line), ethanol (green line) and isopropanol (orange line). (b) Birefringence values obtained from the position of the poles and ceros of $R(\lambda)$ for empty pores (gray), pores filled with water (blue), ethanol (green) and isopropanol (orange).

As it was expected from the results shows in Section 2, a decrease in the birefringence is clearly seen when the refractive index of the liquids that fills the pores increases. Also we can see that for larger wavelengths both the birefringence and its change are smaller than the ones obtained at shorter wavelength, due to the fact that silicon refractive index decreases with the wavelength. At a wavelength of 808 nm we measured birefringence values of 0.120, 0.084, 0.081, 0.079 for pores filled with air, water, ethanol and isopropanol respectively. The sensitivity in terms of phase retardation is 35.47 rad/RIU corresponding to a blue-shift of 755 nm/RIU. At a wavelength of 1500 nm the birefringence values are slightly smaller than the ones at 808 nm, 0.108, 0.074, 0.071 and 0.070. The sensitivity in terms of phase retardation is 17.89 corresponding to a blue-shift of 1407 nm/RIU.

4.2 PSi made from (100) substrate

In this type of samples the phase retardation at normal incidence is almost zero, In so another experimental setup for obtaining the birefringence of the samples, different from the one used in the (110) PSi, has to be used. In this case the phase retardation was measured as a function of the incidence angle of a monochromatic light source. Thus, the output light from a laser is linearly polarized at 45° with respect to the horizontal direction. Then, the linearly polarized light passes through the PSi sample which is mounted on a rotation stage that allows changing the incidence angle of the light at the sample. When the linearly polarized light passes through the sample its main components experience a phase shift that is converted into an amplitude shift by placing a second polarizer (analyzer). Finally, the light intensity is measured by means of a photodiode. Again, similarly to the case of the (110) sample, the phase retardation is obtained by measuring the ratio between the intensity of the light when the polarizer are placed crossed and parallel. The phase retardation is related to the sample birefringence and the incidence angle by:

$$\Delta\phi(\alpha) = \frac{2\pi}{\lambda} \cdot (d_e(\alpha) \cdot \eta_e(\alpha) - d_o(\alpha) \cdot \eta_o(\alpha)) \quad (6)$$

where λ is the incident wavelength of light, and d_e , d_o , η_e , η_o are given by the following equations:

$$d_{e,o}(\lambda, \alpha) = \frac{d}{\sqrt{1 - \frac{\sin^2 \alpha}{n_{e,o}^2(\alpha)}}}; \quad \eta_e(\alpha) = \frac{1}{\sqrt{\frac{\sin^2 \alpha}{n_e^2} + \frac{\cos^2 \alpha}{n_o^2}}}; \quad \eta_o(\alpha) = n_o; \quad (7),(8),(9)$$

where d the PSi membrane thickness, α the rotation angle of the sample and n_e , n_o the ordinary and extraordinary refractive index.

Using the previously described setup the phase retardation was measured as a function of the light incidence angle on the sample first using a 808 nm laser and then using a 1500 nm laser. Figure 5 (a) shows the measured phase retardation at a wavelength first cited wavelength and Figure 5 (b) depicts the results using a 1500 nm laser. In both cases the phase retardation were measured when the pores were filled with air (gray lines), and after immersing the sample in the same liquids that the (110) PSi sample was, that is water (blue lines), ethanol (green lines) and isopropanol (orange lines). The birefringence were obtained by fitting the measured data with the theoretical ones given by Equation 6 having values of 0.044, 0.0201, 0.019, 0.018 at 808 nm and 0.041, 0.020, 0.019, 0.017, at 1500 nm for the sample being filled with air, water, ethanol and isopropanol respectively. The sensitivity in terms of phase retardation at 808 nm for an incidence angle of light of 45° is 9.62 rad/RIU corresponding to a blue-shift of 204 nm/RIU. At a wavelength of 1500 nm the sensitivity value is 4.86 rad/RIU corresponding to a blue-shift of 382 nm/RIU.

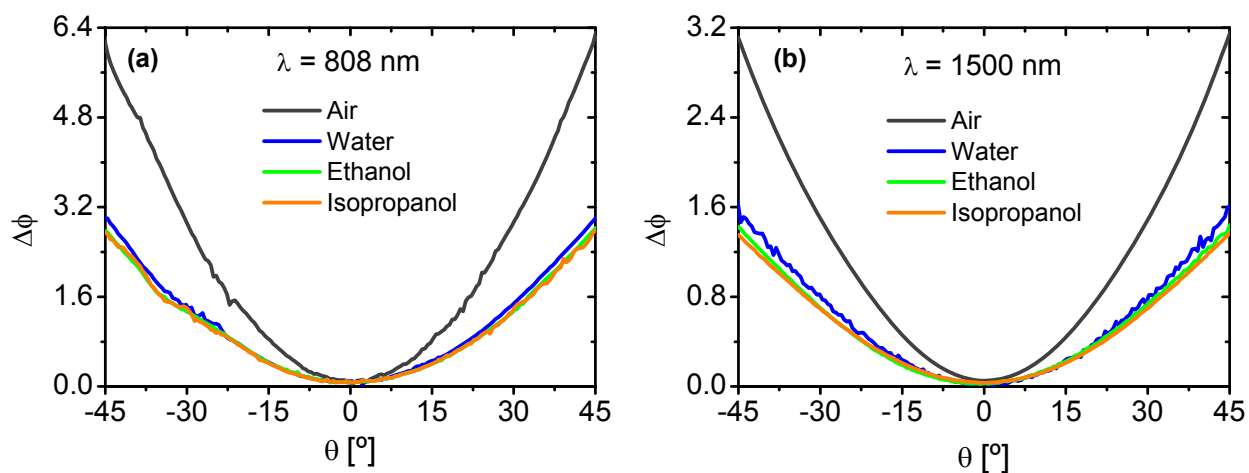


Figure 5. (a) Phase retardation as a function of the light incidence angle for pores filled with air (gray line), water (blue line), ethanol (green line) and isopropanol (orange line) at the wavelengths of 808 nm (a) and 1500 nm (b).

4.3 Comparison

Lastly, we compared the birefringence and sensitivity of the both type of samples at the wavelengths of 808 nm and 1500 nm. Beginning with the values of birefringence, we obtained that the theoretical values of the birefringence were higher in the (100) sample. On the contrary, the experimental results show the opposite behavior: higher birefringence for the (110) samples. These results comes from the ideal modeling of the (100) structure and its difference with the real structure of the fabricated samples where branches of the pores are observed which contributed to homogenize the sample and so to reduce the birefringence. The changes in the phase retardation as a result of filling both types of samples with liquids having different refractive index are shown in Figure 6. We can observe that the higher birefringence change (and so higher sensitivity) were obtained with the (110) samples due to its highest birefringence. On the other hand, since the phase retardation is proportional to the inverse of the wavelength we see that always the phase retardation change is always higher at shorter wavelengths. So we can conclude that to achieve the highest sensitivities using porous silicon as an optical sensor shorter wavelengths are better if one measures the phase retardation shift; on the contrary if the measure the blue-shift in the spectra, longer wavelengths give better sensitivities.

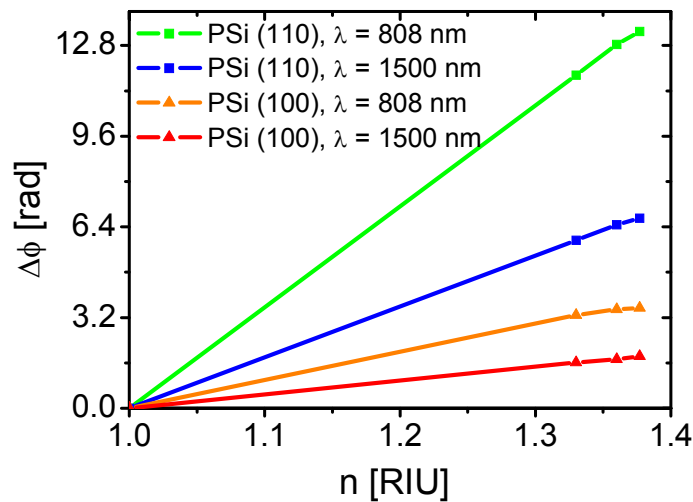


Figure 6. Phase retardation shift as a function of the material that fills the pores for the following cases: PSi sample fabricated from (110) surface oriented silicon at the wavelengths of 1500 nm (green line) and at 808 nm (blue line); PSi sample fabricated from (100) surface oriented silicon at the wavelengths of 1500 nm (orange line) and at 808 nm (red line).

5. CONCLUSION

The modeling, fabrication and characterization of PSi membranes from both (110) and (100) silicon was reported. Based on the Bruggeman model the theoretical birefringence and sensitivity was obtained as a function of the porosity and wavelength, with both values have a maximum shown for porosities around 0.5. The impact that the oxidation of pore walls has on birefringence and sensitivity was also studied theoretically. Thereafter a set of PSi samples from different oriented substrates fabricated and characterized. Porous silicon made from (110) shown to be higher values of birefringence than the ones obtained from a (100) surface oriented silicon. Due to the highest birefringence, also the better sensitivity is found in the (110) samples, measuring a value as high as 1407 nm/RIU at a wavelength of 1500 nm.

REFERENCES

- [1] A. Jane, R. Dronov, A. Hodges, and N.H. Voelcker, "Porous silicon biosensors on the advance," *Trends Biotechnol.*, **27**(4), 230-239 (2009).
- [2] V.S. Lin, K. Motesharei, K.P. Dancil, M.J. Sailor, and M.R.A. Ghadiri, "Porous Silicon-Based Optical Interferometric," *Biosens. Sci.*, **278**(5339), 840-843 (1997).
- [3] V.Mulloni, and L. Pavesi, "Porous silicon microcavities as optical chemical sensors," *Appl. Phys. Lett.*, **76**(18), 2523-2525 (2000).
- [4] M.S. Salem, M.J. Sailor, K. Fukami, T. Sakka, and Y.H. Ogata, "Sensitivity of porous silicon rugate filters for chemical vapor detection," *J. Appl. Phys.*, **103**(8), 083516 (2008).
- [5] T. Jalkanen, V. Torres-Costa, J. Salonen, M. Björkqvist, E. Mäkilä, J. Martínez-Duart, and V. Lehto, "Optical gas sensing properties of thermally hydrocarbonized porous silicon Bragg reflectors," *Opt. Express*, **17**(7), 5446-5456 (2009).
- [6] E. Gross, D. Kovalev, N. Künzner, V.Y. Timoshenko, J. Diener, and F. Koch, "Highly sensitive recognition element based on birefringent porous silicon layers," *J. Appl. Phys.*, **90**(7), 3529-3532 (2001).
- [7] O.B. Hoan R. Liu, Y.Y. Li, M. Sailor, and Y. Fainman, "Vapor sensor realized in an ultracompact polarization interferometer built of a freestanding porous-silicon form birefringent film," *IEEE. Photonic. Tech. L.*, **15**(6), 834-836 (2003).

- [8] J. Álvarez, P. Bettotti, I. Suárez, N. Kumar, D. Hill, V. Chirvony, L. Pavesi, and J. Martínez-Pastor, "Birefringent porous silicon membranes for optical sensing," *Opt. Express* 19, 26106-26116 (2011).
- [9] M. Kompan, J. Salonen, and I. Shabanov, "Anomalous birefringence of light in free-standing samples of porous silicon," *J. Exp. Theor. Phys.*, 90, 324-329 (2000).
- [10] V. Kochergin M. Christophersen, H. Foll, "Effective medium approach for calculations of optical anisotropy in porous materials" *Appl. Phys. B*, 79, 731-739 (2004).
- [11] O. Bisi, S. Ossicini, and L. Pavesi, "Porous silicon: a quantum sponge structure for silicon based optoelectronics," *Surf. Sci. Rep.*, 38(1-3), 1-126 (2000).
- [12] N. Künzner, J. Diener, E. Gross, D. Kovalev, V.Y. Timoshenko, and M. Fujii, "Form birefringence of anisotropically nanostructured silicon," *Phys. Rev. B*, 71(19), 195304 (2005).
- [13] V.Y. Timoshenko, L.A. Osminkina, A.I. Efimova, L.A. Golovan, P.K. Kashkarov, D. Kovalev, N. Künzner, E. Gross, J. Diener, and F. Koch, "Anisotropy of optical absorption in birefringent porous silicon," *Phys. Rev. B*, 67(11), 113405 (2003).
- [14] R.L. Smith, and S.D. Collins, "Porous silicon formation mechanisms," *J. Appl. Phys.*, 71(8), 1-22 (1992).
- [15] Lutich, A.A., Danailov, M.B., Volchek, S., Yakovtseva, V.A., Sokol, V.A., Gaponenko, S.V., "Birefringence of nanoporous alumina: dependence on structure parameters", *Applied Physics B: Lasers and Optics*, 84,1, 327-331, (2006)
- [16] T.C. Choy, "Effective Medium Theory, Principles and Applications," Oxford University Press, (1999).
- [17] K.A. Kilian, T. Bocking, and J.J. Gooding, "The importance of surface chemistry in mesoporous materials: lessons from porous silicon biosensors," *Chem. Commun.*, 630-640 (2009).
- [18] I. Suárez, V. Chirvony, D. Hill, and J. Martínez-Pastor, "Simulation of surface-modified porous silicon photonic crystals for biosensing applications," *Phot. Nano. Fund. Appl.*, doi:10.1016, (2011)
- [19] M. Ghulinyan, C.J. Oton, G. Bonetti, Z. Gaburro, and L. Pavesi, "Free-standing porous silicon single and multiple optical cavities," *J. Appl. Phys.*, 93(12), 972 (2003).